**Supporting Information for:**

Vapor Wall Deposition in Chambers: Theoretical Considerations

Renee C. McVay, Christopher D. Cappa, John H. Seinfeld*

*Correspondence to John H. Seinfeld, seinfeld@caltech.edu

Contents: Figures S1-S7

## Comparison to Zhang et al. (*1*)

The SOA growth data from Zhang et al. (*1*) can be plotted similarly to Figure 3 to observe the competing effects of kinetic limitations and vapor wall deposition. The yields over the course of each toluene low-$NO_x$ photooxidation experiment in (*1*) are shown as circles in Figure S2 as a function of $C_{OA}$ for different seed surface areas. The lines in Figure S2 are yields calculated using the SOM model with parameters fit to the experimental data at each surface area but in the absence of vapor wall deposition (see *SI* of (*1*) for more details). Yields over the course of one representative experiment from Ng et al. (*2*) are shown as diamonds for comparison. The measured yields from Zhang et al. (*1*) quickly reach a plateau with respect to $C_{OA}$, indicating that the SOA formed via the low-$NO_x$ pathway is essentially nonvolatile for $C_{OA} > 10\ \mu g\ \mathrm{m}^{-3}$. These yield curves clearly diverge at different surface areas, due to both vapor wall deposition and kinetic growth limitations. Yields calculated in the absence of vapor wall deposition diverge into separate curves solely as a result of kinetic limitations on particle growth. These yields are higher than the measured yields because species that would have otherwise condensed to the walls are able to partition to particles. The model presented here qualitatively reproduces this behavior, Figure S3. To match the nonvolatile behavior observed in the low-$NO_x$ case of (*1*), the saturation concentrations of species B through D are all decreased to $10^{-3}\ \mu g\ \mathrm{m}^{-3}$. The magnitudes of the yields clearly differ from (*1*), but the general behavior is reproduced.

Yields over the course of each toluene high-$NO_x$ photooxidation experiment in (*1*) are shown in Figure S4, circles representing observed yields and lines representing calculated yields from the SOM model in the absence of vapor wall deposition. Although the yield curves as a function of $C_{OA}$ do diverge slightly, the effect is much less pronounced than in the low-$NO_x$ case. Furthermore, the yields do not reach a plateau with respect to $C_{OA}$. To match this observed behavior, Figure S5, the saturation concentrations of species B through D are set as $[10^3\ 10^1\ 10^{-1}]\ \mu\mathrm{g\ m}^{-3}$. The reaction rate constants are set as $k[\mathrm{OH}]_{A\rightarrow B} = k[\mathrm{OH}]_{B\rightarrow C} = 5\mathrm{x}10^{-5}\ \mathrm{s}^{-1}$ and $k[\mathrm{OH}]_{C\rightarrow D} = 5\mathrm{x}10^{-4}\ \mathrm{s}^{-1}$. These parameters do not necessarily represent volatilities or rates of the toluene high-$NO_x$ experiments in (*1*), but merely show that the present model can reproduce the general behavior.

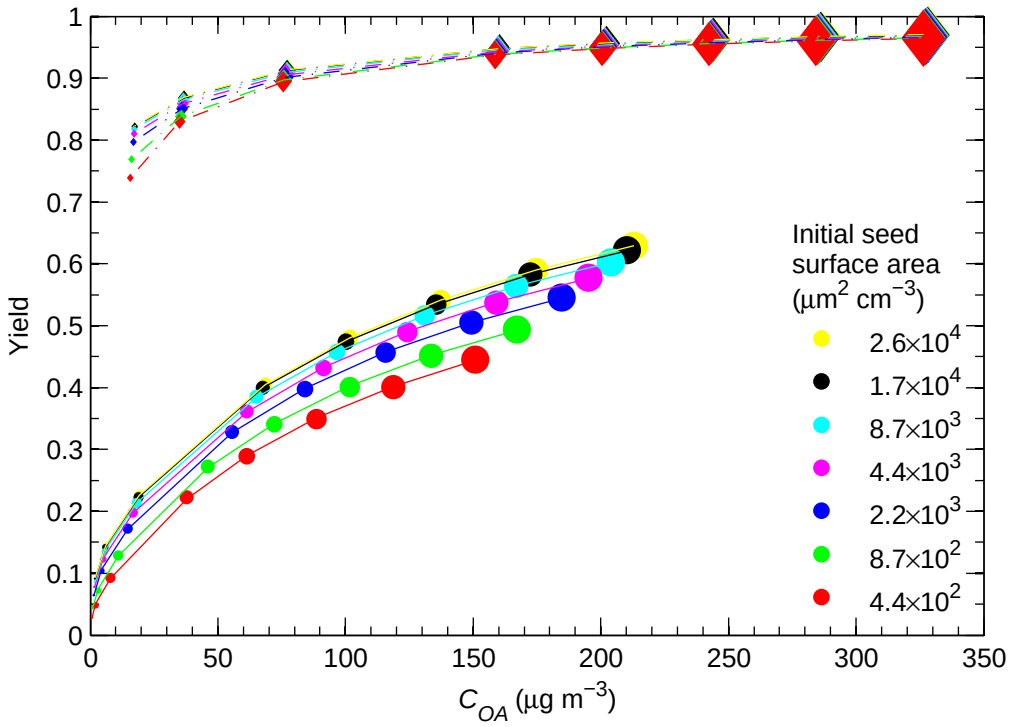


Figure S1: SOA yields after 20 h of simulation as a function of the final organic aerosol concentration $C_{OA}$ for $\alpha_p = 0.01$. The points on the curve were generated by varying the initial parent VOC concentration $G_{A0}$ with (circles) and without (diamonds) vapor wall deposition. The size of the markers increases as $G_{A0}$ increases and colors correspond to different values of the initial seed surface area. The lines were generated by fitting a two-product model to the datapoints.

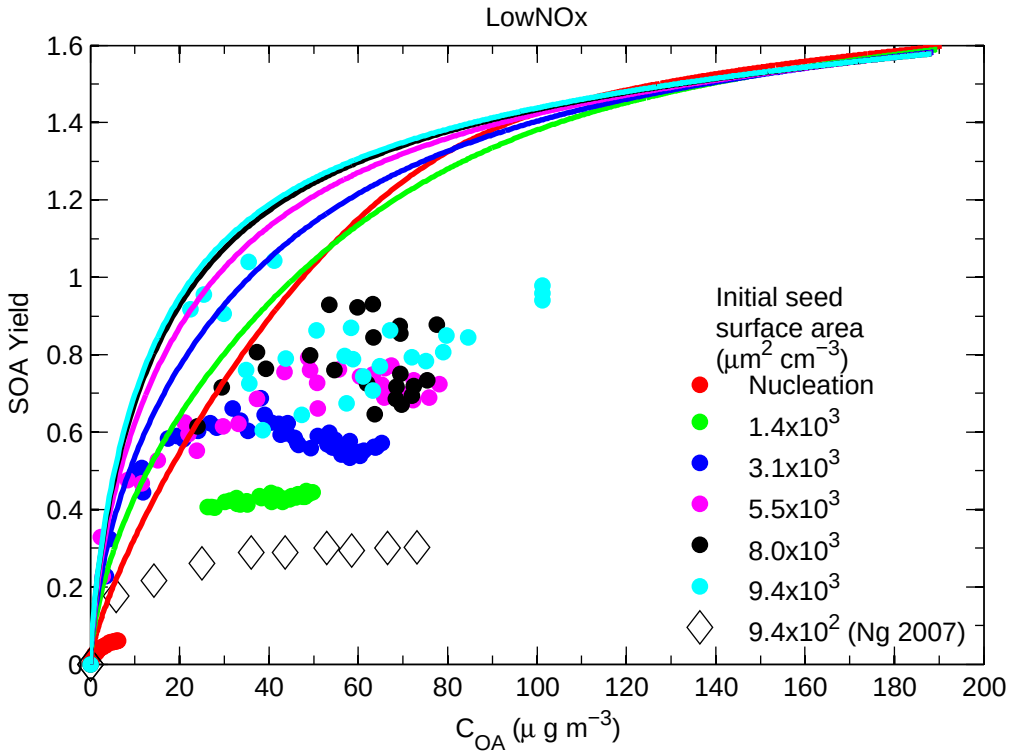


Figure S2: SOA yields over the course of each toluene low-$NO_x$ photooxidation experiment in (*1*) as a function of $C_{OA}$ for different seed surface areas are shown as circles. Lines are yields calculated using the SOM model with wall deposition turned off (see *SI* of (*1*) for more details). Yields over the course of one representative experiment from (*2*) are shown as diamonds for comparison.

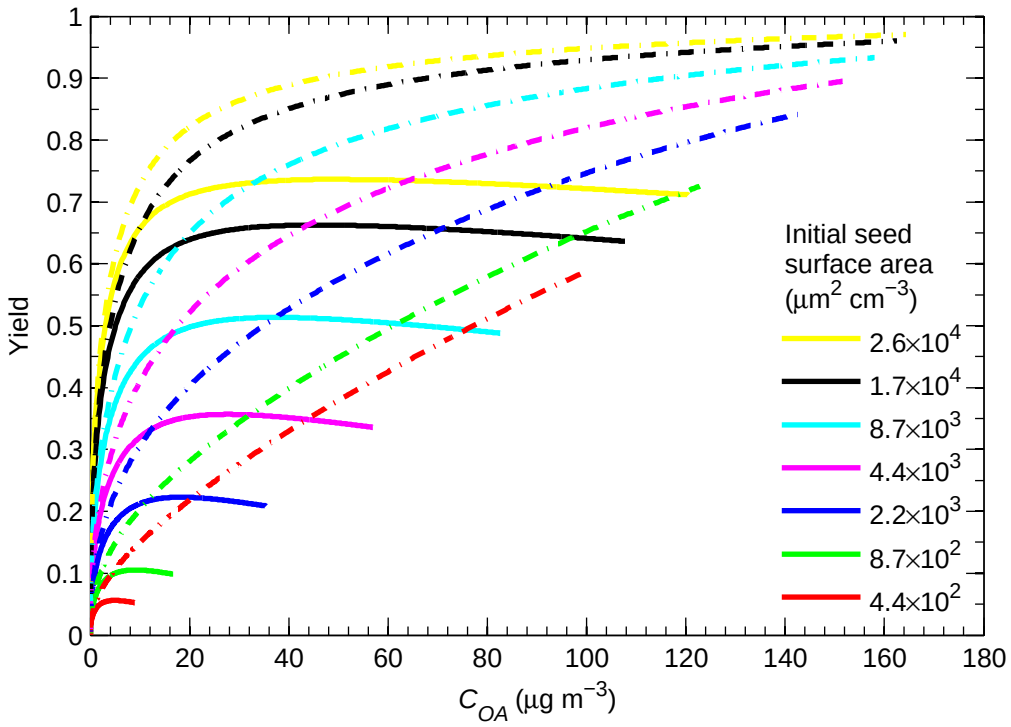


Figure S3: SOA yields are shown as a function of $C_{OA}$ over the course of a simulation using the present model, with $C^*_{B-D} = 10^{-3}$ $\mu$ g m$^{-3}$ and $\alpha_p = 0.001$. Yields are calculated in the presence (solid lines) and absence (dashed lines) of vapor wall deposition. Different initial seed surface areas are shown using different colors.

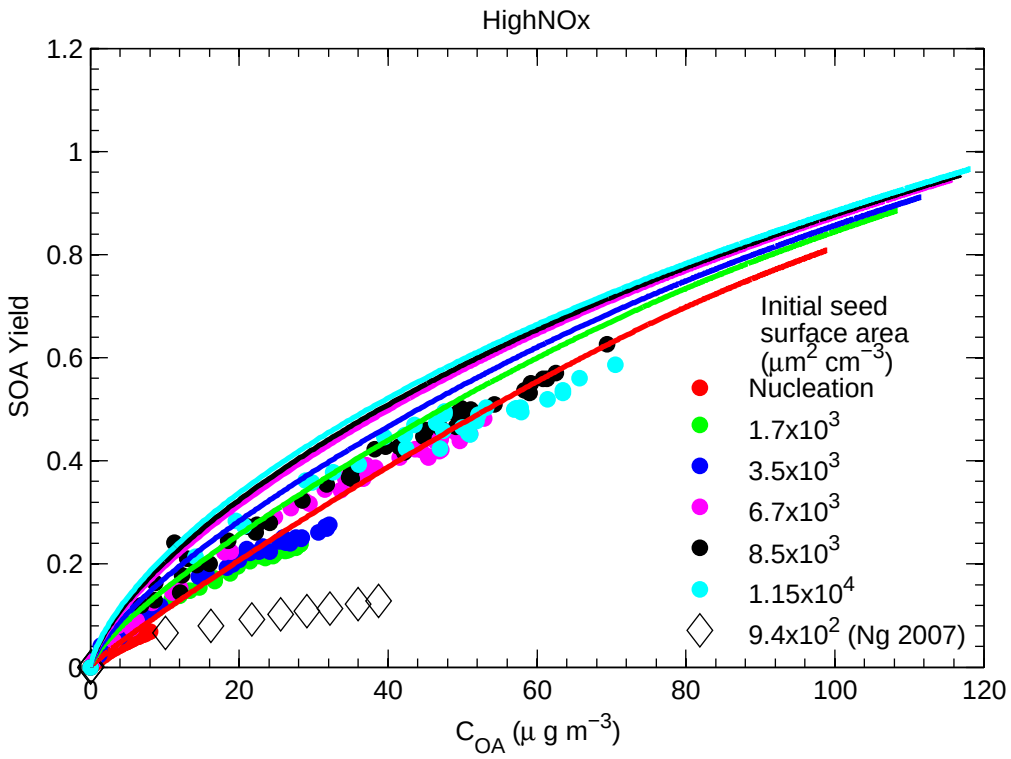


Figure S4: SOA yields over the course of each toluene high-$NO_x$ photooxidation experiment in (*1*) a function of $C_{OA}$ for different seed surface areas are shown as circles. Lines are yields calculated using the SOM model with wall deposition turned off (see *SI* of (*1*) for more details). Yields over the course of one representative experiment from (*2*) are shown as diamonds for comparison.

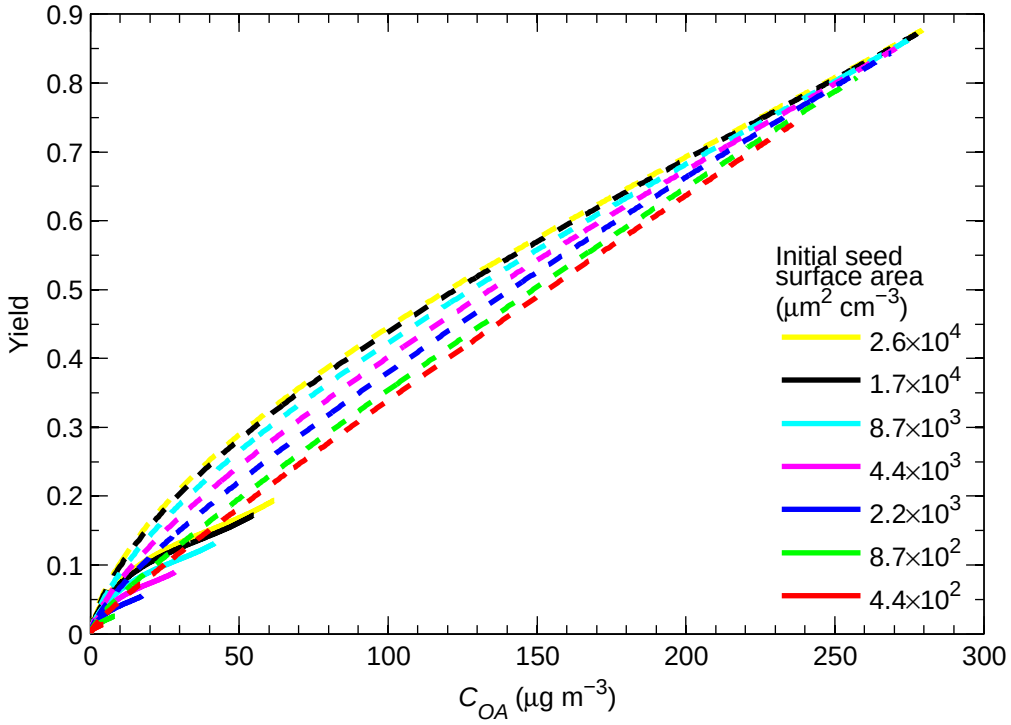


Figure S5: SOA yields are shown as a function of $C_{OA}$ over the course of a simulation using the present model, with $C_i^*$ = [$10^3$ $10^1$ $10^{-1}$] $\mu$g m$^{-3}$, $k[\mathrm{OH}]_{A\rightarrow B} = k[\mathrm{OH}]_{B\rightarrow C} = 5\mathrm{x}10^{-5}$ s$^{-1}$ and $k[\mathrm{OH}]_{C\rightarrow D} = 5\mathrm{x}10^{-4}$ s$^{-1}$, and $\alpha_p = 0.001$. Yields are calculated in the presence (solid lines) and absence (dashed lines) of vapor wall deposition. Different initial seed surface areas are shown using different colors.

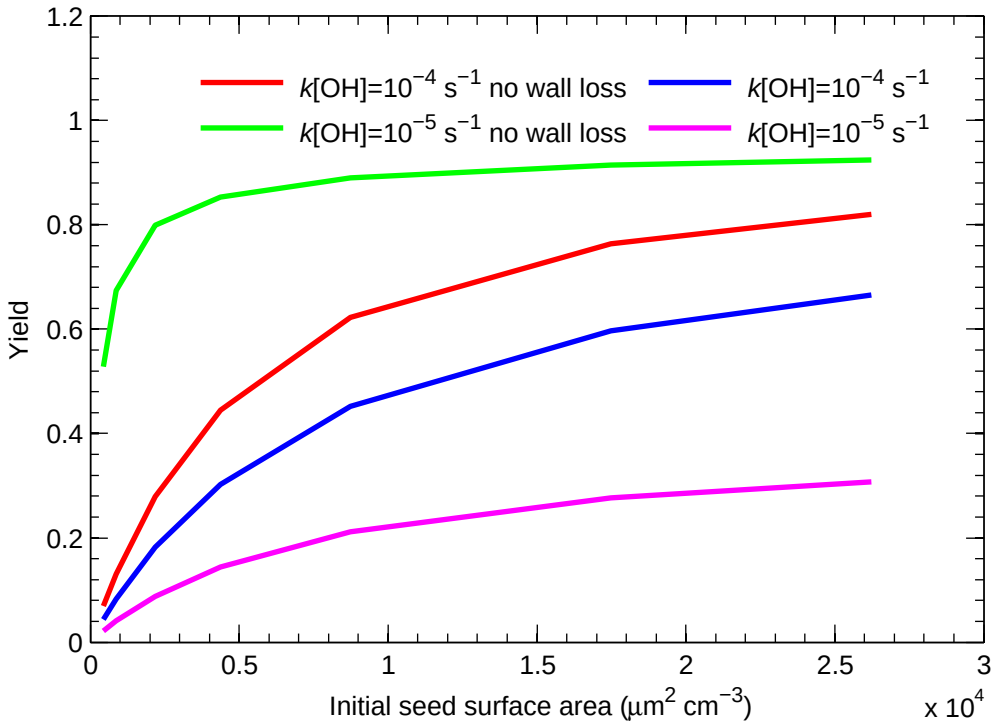


Figure S6: SOA yields after an equivalent amount of OH exposure (20 h for $k[\mathrm{OH}]_{A\rightarrow B} = 10^{-5}$ s$^{-1}$ and 2 h for $k[\mathrm{OH}]_{A\rightarrow B} = 10^{-4}$ s$^{-1}$) as a function of the final organic aerosol concentration $C_{OA}$ for simulations with $\alpha_p = 0.001$ for different values of $k[\mathrm{OH}]_{A\rightarrow B}$, with and without vapor wall deposition.

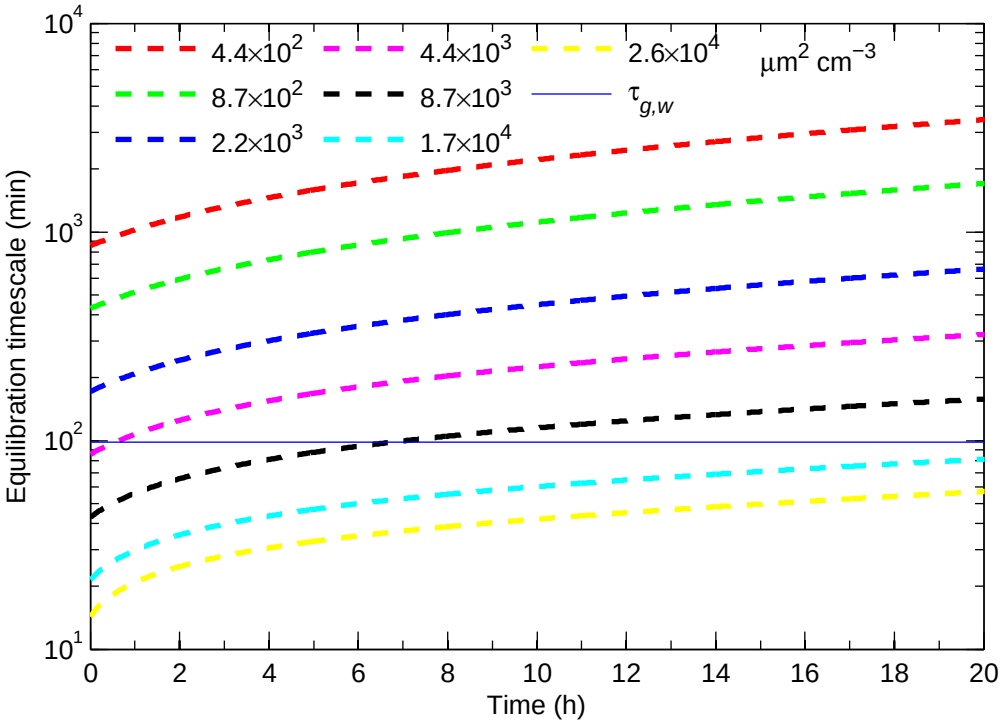


Figure S7: Time evolution of equilibration timescale for gas-particle partitioning $\tau_{g,p}$ for different initial seed surface areas. The equilibration timescale for gas-wall partitioning ($\tau_{g,w} = 1/k_{wall,on}$) is shown as a horizontal line because this timescale does not change with time.

## References

(1) Zhang, X.; Cappa, C. D.; Jathar, S. H.; McVay, R. C.; Ensberg, J. J.; Kleeman, M. J.; Seinfeld, J. H. Influence of vapor wall-loss in laboratory chambers on yields of secondary organic aerosol. *Proc. Natl. Acad. Sci.* **2014**, *111*, 5802–5807, doi:10.1073/pnas.1404727111.

(2) Ng, N. L.; Kroll, J. H.; Chan, A. W. H.; Chhabra, P. S.; Flagan, R. C.; Seinfeld, J. H. Secondary organic aerosol formation from *m*-xylene, toluene, and benzene. *Atmos. Chem. Phys.* **2007**, *7*, 3909-3922.